

SDRP Journal of Earth Sciences & Environmental Studies (ISSN: 2472-6397)

The Spatiotemporal Distribution of PM_{2.5} and its Relationship to Land-Use Patterns and Special to Land-Use and People in Hangzhou

DOI: 10.25177/JESES.3.2.6

Research

Received Date: 15th Jun 2018Accepted Date: 23rd Jul 2018Published Date: 30th Jul 2018

Copy rights: © This is an Open access article distributed under the terms of International License.



CORRESPONDENCE AUTHOR

Li Tian

Qianyanzhou Ecological Research Station, Key Laboratory of Ecosystem Network Observation and Modeling, Institute of Geographic Sciences and Natural Resources Research, Chinese Academy of Sciences, Beijing, China

Email: tianli@igsnr.ac.cn

CITATION

Li Tian, The Spatiotemporal Distribution of PM_{2.5} and its Relationship to Land-Use Patterns and Special to Land-Use and People in Hangzhou(2018)SDRP Journal of Earth Sciences & Environmental Studies 3(3)

ABSTRACT:

Assessments have quantified the burden of air pollution at the national scale in China; air quality managers would benefit from assessments that disaggregate health impacts over regions and time. The air quality in Hangzhou City, which is one of the central cities of the Yangtze River Delta Urban Agglomeration, was not in great condition. We used the monitoring sites data and MODIS remote-sensing Aerosol optical thickness (AOT) for the inversion of the PM_{2.5} concentration map for all four seasons in 2015. Next, we combined the land use data, population density data, and school data (kindergarten, primary school, and middle school) to analyze their correlation; we found that the seasonal variation characteristics of PM_{2.5} concentration distribution was winter > spring > autumn > summer. For the different land use type in winter and spring, 59.86% and 56.62% land area showed the PM_{2.5} > 50 μg/m³, respectively. In autumn, 54.38% of the land area exposure was PM_{2.5} 35~50 μg/m³. In summer, the PM_{2.5} concentration was lowest, at 70.01%, and the land surface area showed PM_{2.5} < 35 μg/m³. Increasing the forest landscape performs the function of absorbing and filtering the par-

ticulate air pollution, resulting in high PM_{2.5} concentration at this landscape. It was also discovered that only 9.06% of the population lived in an environment that met the national air quality standards. Specifically, only 1.66% (14,055) of infants and juveniles were living in PM_{2.5} < 35 μg/m³. Considering the lag health effects of long-term PM_{2.5} exposure, it is necessary to track these infants' and juveniles' health conditions from now until they enter into adulthood. This should enable us to more effectively eliminate the PM_{2.5} that is harmful to our health. We firmly believe that not only in Hangzhou, but also spanning all of China, many infants and juveniles live in a severely polluted environment in which we need to pay close attention, as their future health is directly relative to the future prosperity of the country as a whole.

Keywords: PM_{2.5}; spatial and temporal variations; Land surface landscape; infants and juveniles

1. INTRODUCTION

In the haze days, PM_{2.5} particle concentration occupied about 56.7%~75.4% of the total suspended particles and accounted for more than 80%~90% of PM₁₀ (the particles measured ≤ 10 μm in diameter of aerody-

namics) [1]. The high exposure of babies to PM_{10} turned out to be one of the primary causes of decreased head and body size [2], and the long-term exposure to high concentrations of $PM_{2.5}$ was associated with serious health complications including stroke, ischemic heart disease, chronic obstructive pulmonary disease (COPD), lung cancer (LC), and acute lower respiratory infection (ALRI) [3-10]. Ambient fine particulate matter ($PM_{2.5}$) pollution ranked sixth among all risk factors for global premature mortalities and disability-adjusted life-years (DALYs) [11, 12]. Song, et al. [13] used the national air quality monitoring stations in 367 cities in China between the years 2014 and 2016, which resulted in the population's attributable mortality rate (10-5 y-1) showing 112.0 in the current year analysis, and 124.3 in a 10-year time lag analysis. Considering the lag health effects of long-term $PM_{2.5}$ exposure [13, 14], the health risks of infants and juveniles who live long-term amidst a severely polluted environment would increase drastically; we, as a people, must take responsibility for paying more attention to these potential health risks and improving their overall living environment.

Most PM comes from both rapid industrialization and motorization [15, 16]. The pollution problem spread widely in European and North American cities in the 1950s and 1960s, but has since become more pronounced in developing countries (e.g., India, China) [17, 18]. In China, over the last few decades, rapid economic development has led to worsening air quality [19-21], with nearly none of the population living in areas meeting the World Health Organization (WHO) Air Quality Guidelines (AQG) of $PM_{2.5}$ $10 \mu\text{g}/\text{m}^3$ [22-26]. Between the years 2004-2012, over 93% of people in China lived in areas where $PM_{2.5}$ exceeded China's National Air Quality Standard for Grade II of $35 \mu\text{g}/\text{m}^3$ [27]. This was mainly a result of the quick economic development and population urbanization in China. Land surface properties such as roads, construction, human behavior, and vegetation can directly filter pollutants and indirectly influence the air movement through its heterogeneous urban canopies [28]. A better and clearer understanding of spatial and temporal variations of $PM_{2.5}$ can contribute to the population's effective exposure to a differ-

ent $PM_{2.5}$ concentration, and then subsequently the adoption of effective measures to mitigation harm by air pollution will follow.

The often-used approaches for estimating $PM_{2.5}/PM_{10}$ concentration are either based on remote-sensing data or are derived from monitor-based data. We know the profile of aerosol particle liquidity in space; with the sparse discontinuity of the ground environment observation station, it is difficult to reveal both aerosol particles' spatial and temporal distributions as well as transmission characteristics in a wide space [29]. Aerosol optical thickness (AOT) data obtained from the Moderate Resolution Imaging Spectroradiometer has been proven to be a potentially useful predictor of $PM_{2.5}$ concentrations [30, 31]. However, due to dissimilarities in surface characteristics, meteorological conditions, and the aerosol fine mode fraction [32, 33], the application of using AOT as a proxy for reflecting spatial patterns of PM also has limitations [34, 35]. In this case, the combination of the dispersed monitoring sites data and MODIS remote-sensing retrieval could be an effective inversion of the spatiotemporal distribution of $PM_{2.5}$ concentration.

In this study, we are focusing on Hangzhou City, which is one of the central cities of the Yangtze River Delta Urban Agglomeration; we explored its atmospheric environment (Figure 1a) and found that, as a tourist city, Hangzhou City's air quality condition was not in sufficient shape [36-50]. Liu et al. [27] analyzed the atmospheric $PM_{2.5}$ mass concentration variation characteristics in Hangzhou from 2011 to 2014 and concluded that the peak appeared in 2013 ($52.2 \mu\text{g}/\text{m}^3$) and is closely related to the motor vehicle emissions and changes in meteorological conditions. Jin et al. [41] found where the $PM_{2.5}$ particle concentration occurred, including 21.6% caused by automobile fumes, 16.7% caused by burning coal, and 12.2% caused by ash, soil, and concrete buildings. Land use types of urban areas also have a significant impact on the spatial distribution of urban $PM_{2.5}$ [40]. According to the spatial distribution of $PM_{2.5}$ in the region, the reasonable spatial layout of land use type is carried out in combination with weather and terrain conditions, which are conducive to the long-term control of particle pollutants.

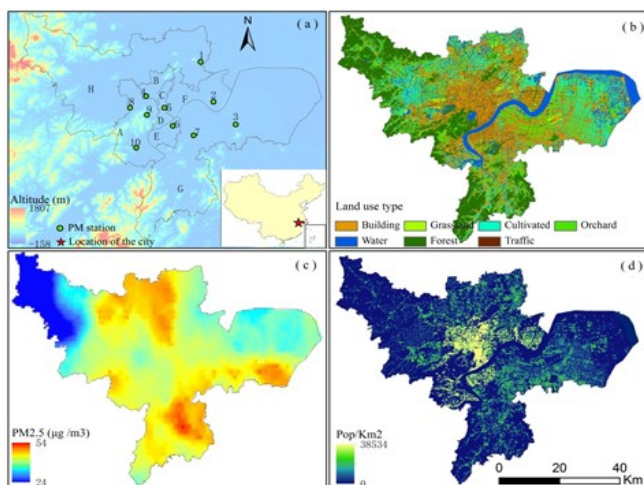


Figure.1 (a) Spatial distribution of 10 $PM_{2.5}$ monitoring stations in the eight study districts (A Xihu; B Gongshu; C Xiacheng; D Shancheng; E Binjiang; F Jianggan; G Xiaoshan; H Yuhang), 1~10 are the monitoring stations; (b) the Land-use map of urban district in Hangzhou; (c) the annual $PM_{2.5}$ concentration spatial distribution in Hangzhou in 2015; (d) the people density spatial distribution in 2015. Km^2 .

In this study, our main objective is as follows: first, to clear spatial and temporal variations of the $PM_{2.5}$ mass concentration on Hangzhou roofing landscapes in 2015; next, to examine the empirical relationships between the spatiotemporal changes of $PM_{2.5}$ and the land use types; next, to analyze the population density distributions exposed to different $PM_{2.5}$ concentrations; and finally, to clear the distribution of schools (kindergarten, primary school, and middle school) under different $PM_{2.5}$ mass concentrations. Our results are aimed toward simplifying the tracking of potential health problems in infants and juveniles into adulthood based on the $PM_{2.5}$ resulting in lagging, long-term health hazards.

2. MATERIALS AND METHODS

2.1. Study Area

Hangzhou city, the capital city of the Zhejiang Province, covers an area of $16,596 km^2$ and includes thirteen districts; this study covers the central main urban area including eight districts: Shancheng, Xiacheng, Jianggan, Gongshu, Xihu, Binjiang, Yuhang, and Xiaoshan (Figure.1a). The study area was $3,376 km^2$, the population density was $2,111.96 Pop/km^2$ in 2015,

and the vehicles were 2.23×10^6 , (<http://www.hzfc.gov.cn/web>). The terrain of the flat, high-west low east has a gentle slope inclination. Hangzhou annually experiences a humid subtropical climate with four distinctive seasons characterized by long, hot, humid summers and chilly, cloudy winters. The average annual precipitation is 1,438 mm, abundant during summer and relatively low during winter. In late summer, Hangzhou suffers from typhoon storms. The prevailing surface winds are main southerly during summer and northerly during winter. The atmospheric structure is relatively stable, and temperature inversion often occurs in late autumn and winter [36].

2.2. Data

2.2.1. $PM_{2.5}$ Data

Terra – MODIS, the atmospheric aerosol optical thickness (AOT) (Collections 5, MOD04-3K) acquired from NASA/GSFC (Goddard Space Flight Center) LAADS (Level 1 and Atmosphere Archive and Distribution System). AOT data was extracted from aerosol particles over land surfaces by $0.55 \mu m$ per day. Validated real-time hourly concentrations of $PM_{2.5}$ from January 2015 to December 2015 in Hangzhou were downloaded from the National Environmental Monitoring Centre (CNEMC, <http://www.cnemc.cn/>) (Figure .1a). Consider the time match with the MODIS AOT as well as the transformational hourly $PM_{2.5}$ station point data that averages daily.

2.2.2. Other Data

For building the model between the whole layer of AOT and the dry particle mass concentration near the ground, one needs vertical correction and humidity correction for the model. All meteorological data comes from reanalysis data by NCEP (<http://dss.ucar.edu/>), including a comprehensive set of observation data covering multiple elements spanning a wide range and an extended period of time.

The land use map supplied by the Second Surveying and Mapping Institute of Zhejiang Province had a scale of 1:10,000 and was manually produced based

on high-resolution aerial photos in 2015 (Figure. 1b). The number of student data and the schools' spatial distribution map was collected by the Hangzhou Education Bureau, and the population data was collected from census data.

2.3. Method

We needed to finish three steps in order to realize the spatial distribution PM_{2.5} concentration (Figure. 2) first at MODIS AOT inversion and calibration; the second step realized the match well between some satellite data and PM_{2.5} monitoring data; the third step involved building regression modeling between PM_{2.5}

monitoring data and the collected satellite data. Based on other papers [51-55], the remote sensing inversion algorithms for the MODIS aerosol optical thickness (AOT) products in this paper adopted dark target algorithm. Second, some effective pixel data was collected that matched well with the satellite transit data. Finally, the geometric mean value of the effective pixel data was used to establish a line regression model between AOT and PM_{2.5} mass concentration. To achieve the AOT and PM_{2.5} regression modeling, the essential step was to finish AOT calibration and water vapor calibration; this approach refers to Levy et al [56], and the simulation process is as follows (Figure. 3).

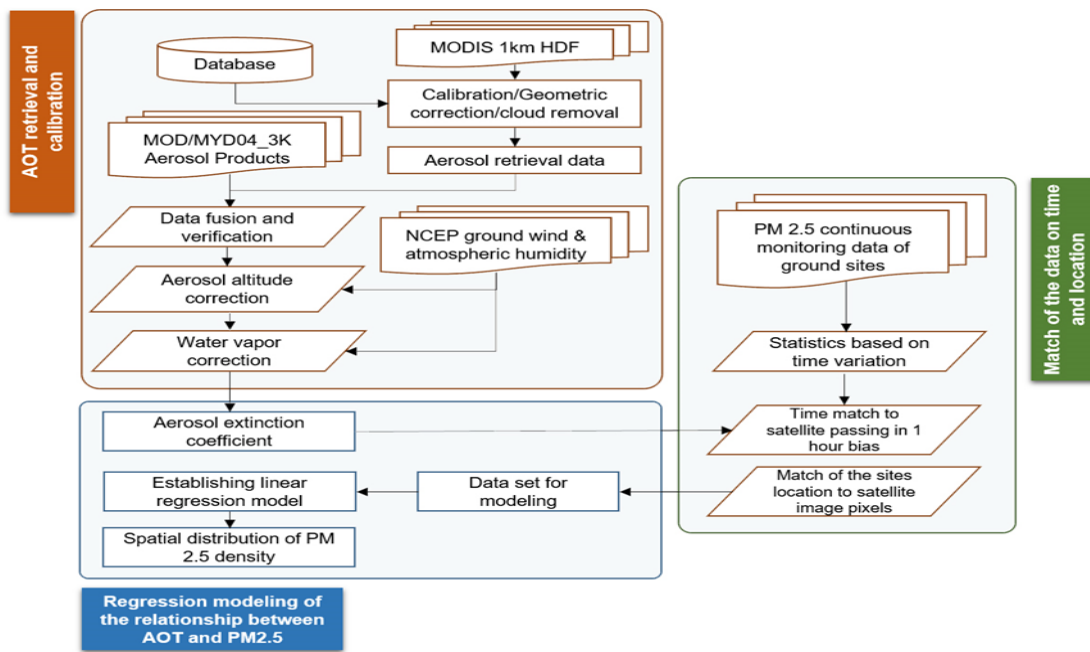


Figure 2. Based on the MODIS Aerosol optical thickness (AOT) inversion spatial PM_{2.5} concentration flow chart

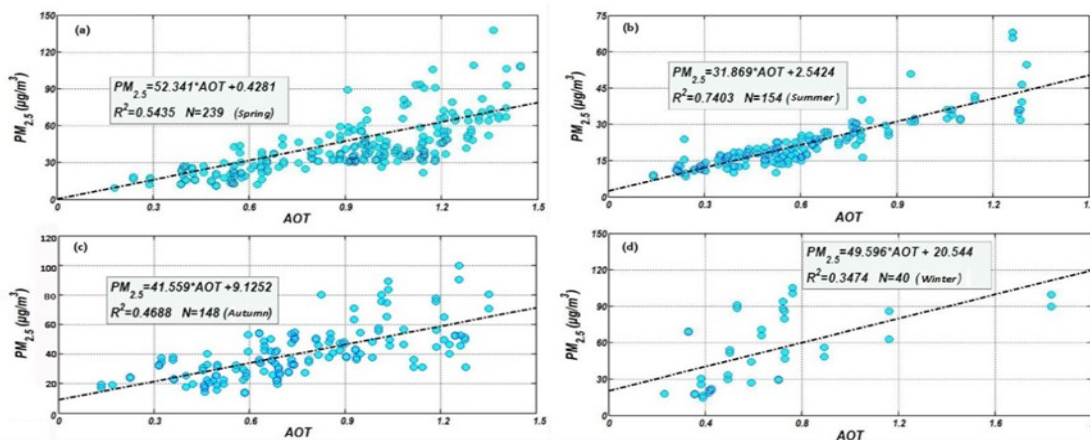


Figure.3 The line regression analysis between AOT and the PM_{2.5} concentration monitor data in the different seasons.

Based on the $PM_{2.5}$ concentration evident in all four seasons and CNEMC standards, we divided the spatial $PM_{2.5}$ concentration into three classes: $<35\mu\text{g}/\text{m}^3$ (non-polluted), $35\text{--}50\mu\text{g}/\text{m}^3$ (intermediate) and $>50\mu\text{g}/\text{m}^3$ (heavy). The year was divided into four seasons based on the standards of the Chinese Meteorological Administration in order to calculate the seasonal mean, minimum, maximum, and standard deviation: spring (March-May), summer (June-August), autumn (September-November), and winter (December-February).

Spatial interpolation was used based on the census data of streets and the building density to generate the population density map in 2015 (Figure. 2d). Then, we analyzed the quantitative relationship between the $PM_{2.5}$ concentration and the land use types in different seasons; the population density and the schools' distribution under the different $PM_{2.5}$ concentration range was significant regarding quantitative analysis.

3. RESULTS AND DISCUSSION

3.1. Line Regression Between AOT and the $PM_{2.5}$ Concentration

After AOT inversion and calibration and water vapor calibration were achieved, the line regression analysis was built between AOT and the $PM_{2.5}$ concentration among the seasons (Figure. 3). It was found that the model fitting correlation was varying in different seasons, the determination coefficient was between 0.347~0.740, and the accuracy order of the model was determined: summer > spring > autumn > winter. This season difference affected by some factors, such as the height of the atmospheric mixing layer in autumn and winter, was very low and was not conducive to the diffusion of air particle pollutants. In addition, in autumn and winter, where cold waves were frequent, the change of weather conditions led to increasing atmospheric pollutant space-time variability and the model fitting accuracy decreased. However, the results of the four seasons modeling met the needs of the article [56].

3.2. The spatiotemporal distribution in $PM_{2.5}$

In Hangzhou, the annual average of $PM_{2.5}$ concentration was $43\mu\text{g}/\text{m}^3$ (std = 5.28). This result displayed that Hangzhou's region air quality was well over 50% ($53.0\mu\text{g}/\text{m}^3$) than that of China in 2015 [13, 27]. Similar to other cities in 2015, Beijing was $80.8\mu\text{g}/\text{m}^3$, Shanghai was $53.9\mu\text{g}/\text{m}^3$, Guangzhou was $38.8\mu\text{g}/\text{m}^3$, and Shenzhen was $29.9\mu\text{g}/\text{m}^3$. The Beijing-Tianjin-Hebei area was $77.1\mu\text{g}/\text{m}^3$, Yangtze River Delta area was $52.9\mu\text{g}/\text{m}^3$, and Pearl River Delta area was $34.4\mu\text{g}/\text{m}^3$ in 2015 (http://www.greenpeace.org/eastasia/Global/eastasia/publications/reports/climate-energy/2015/GPEA%202015%20City%20Rankings_briefing_int.pdf). After 2013 experienced the peak PM value spanning all of China, the $PM_{2.5}$ concentration showed a significant declining trend. Like in Hangzhou, the $PM_{2.5}$ was $52.2\mu\text{g}/\text{m}^3$ in 2013 [43]. However, this measurement still had a long way to go in order to reach China's National Air Quality Standard for Grade II [22]; in China's total 366 cities, over 80% did not reach China's National Air Quality Standard for Grade II limit of $35\mu\text{g}/\text{m}^3$ [57]. For the spatial distribution of the annual average, $PM_{2.5}$ was mainly focused in Gongchu, Shangcheng, Xiacheng, part of Xihu, Yuhang, and Xiaoshan (Figure. 1C). The mean $PM_{2.5}$ concentration was $50.27\mu\text{g}/\text{m}^3$ (std = 7.32) in spring, $24.87\mu\text{g}/\text{m}^3$ (std = 4.40) in summer, $43.63\mu\text{g}/\text{m}^3$ (std = 5.66) in autumn, and $53.19\mu\text{g}/\text{m}^3$ (std = 6.92) in winter (Figure. 4a-d). Regarding spatial distribution, the lowest values all showed up in the northwest mountainous area (Figure. 4). Compared with the season variation of $PM_{2.5}$, the result for spatial distribution was winter > spring > autumn > summer. The seasonal characteristics of $PM_{2.5}$ concentration were consistent with the ground observation results in Hangzhou, and this year's variation was consistent with other cities, as well [58-62]. In winter, air pollution was still a serious issue that severely affected people's lives in China, and the administrative department continued struggling to find efficient ways to send this atmospheric pollution into remission.

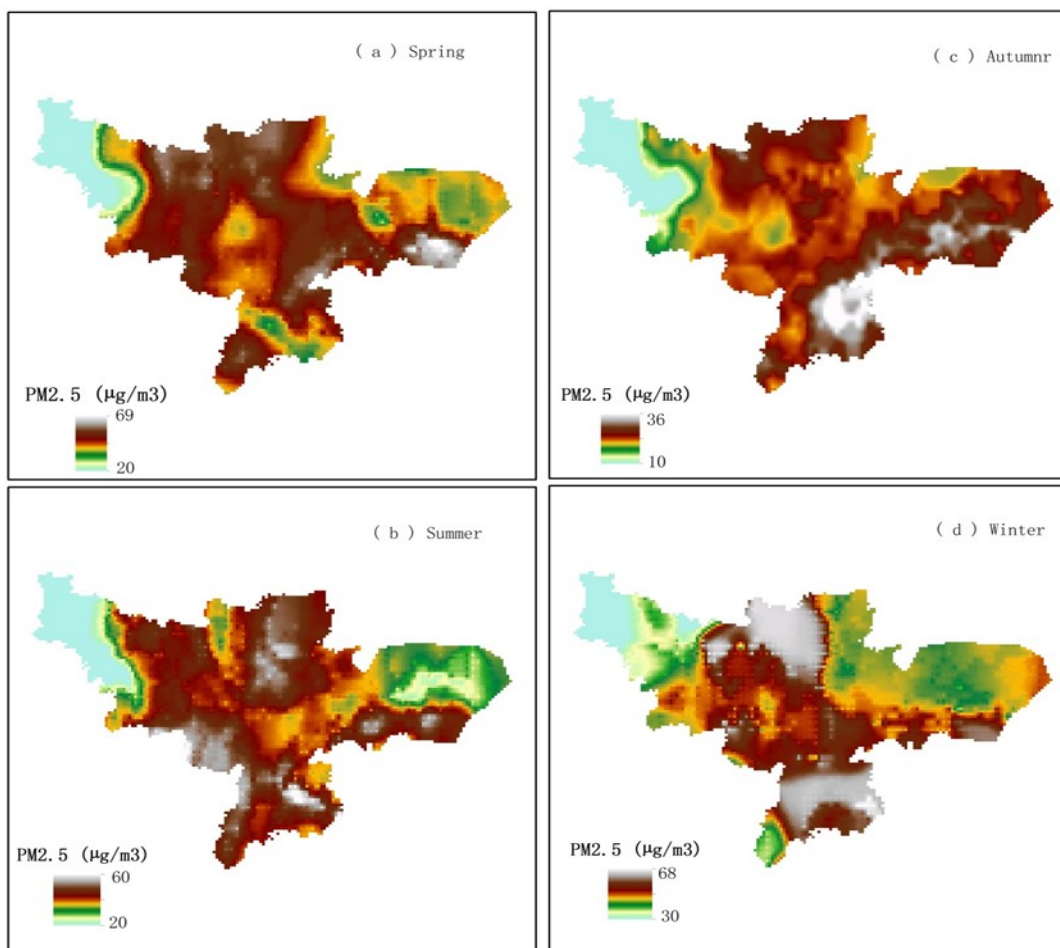


Fig 4. The $PM_{2.5}$ concentration spatial distribution in four seasons in Hangzhou.

Among a study of eight districts in four seasons, the Xiacheng district showed three seasons with the highest mean value (Figure. 4, Table 1); the values equaled $54.10 \mu\text{g}/\text{m}^3$ in spring, $29.73 \mu\text{g}/\text{m}^3$ in summer, and $45.27 \mu\text{g}/\text{m}^3$ in autumn. The Gongshu district showed the highest value in winter, which was $61.08 \mu\text{g}/\text{m}^3$. The lowest mean value $PM_{2.5}$ concentration for all four seasons appeared in the Yuhang district: the values were $47.65 \mu\text{g}/\text{m}^3$ in spring, $23.31 \mu\text{g}/\text{m}^3$ in summer, $39.41 \mu\text{g}/\text{m}^3$ in autumn, and $54.63 \mu\text{g}/\text{m}^3$ in winter. Interestingly, the Xiaoshan district showed the largest maximum value in all four seasons, with $68.54 \mu\text{g}/\text{m}^3$ in spring, $35.95 \mu\text{g}/\text{m}^3$ in summer, $59.63 \mu\text{g}/\text{m}^3$ in autumn, and $67.97 \mu\text{g}/\text{m}^3$ in winter (Table 1). Additionally, the spatial distribution showed multiple “hot areas” in all four seasons (Figure. 4).

3.3. Correlation analysis between land use and the spatial distribution of $PM_{2.5}$ concentration

For the seven land types in the study area, the building area occupied 26.86% (905.84km^2), the water area was 12.87% (434.22km^2), the grassland was 4.94% (166.23km^2), the forest area was 26.31% (887.42km^2), cultivated land was 11.95% (403.07km^2), traffic land was 5.38% (181.53km^2), and orchard land was 11.67% (393.91km^2) (Figure. 1b). We gathered statistics for the area percentage of seven land use types according to the three classes of $PM_{2.5}$ concentration (Table 2). The resulting data concluded that in spring, at $PM_{2.5} < 35 \mu\text{g}/\text{m}^3$, the land surface area accounted for 4.16%; at $PM_{2.5}$ between $35 \sim 50 \mu\text{g}/\text{m}^3$, the land surface area accounted for 39.23%, and at $PM_{2.5} > 50 \mu\text{g}/\text{m}^3$, the land surface area accounted for 56.62%. During summer, at $PM_{2.5} < 35 \mu\text{g}/\text{m}^3$ the land area accounted for 70.01%, between $35 \sim 50 \mu\text{g}/\text{m}^3$ the land surface area accounted for 30%,

and no area accounted for $> 50\mu\text{g}/\text{m}^3$. During autumn, the $<35\mu\text{g}/\text{m}^3$ area only accounted for 5.17%, 54.38% was between $35\sim 50\mu\text{g}/\text{m}^3$, and was 40.44 was $> 50\mu\text{g}/\text{m}^3$. For winter, 59.86% land area was $>50\mu\text{g}/\text{m}^3$, 34.84% land area was between $35\sim 50\mu\text{g}/\text{m}^3$, and only 5.28% land area was $< 35\mu\text{g}/\text{m}^3$. For the different land types, the forest area accounted for the largest proportion. Ranking below $35\mu\text{g}/\text{m}^3$ $\text{PM}_{2.5}$ concentration, the values were 3.49% in spring, 23.39% in summer, 3.93% in autumn, and 4.35% in winter. Interestingly, the forest land type measured $\text{PM}_{2.5}$ between $35\sim 50\mu\text{g}/\text{m}^3$. In spring, autumn, and winter, the largest area proportion was calculated at 13.76%, 15.49% and 14.81%, respectively; in summer, the largest area proportion was building land (24.12%).

For the building land type, spring, autumn, and winter showed the largest area proportion of the $\text{PM}_{2.5}$ $>50\mu\text{g}/\text{m}^3$ (Table 2). The building land means more population activities, which resulted in more air pollution sources [27]. The forest type had a high vegetation roof cover; however, it occupied the high area proportion in $\text{PM}_{2.5}$ between $35\sim 50\mu\text{g}/\text{m}^3$. The main reason for this result was that, as air moves through the forest landscape, the filtering of particulate air pollution results in higher pollutants within forests and other green spaces [17, 63, 64]. Janhäll [28] has advocated that increasing the vegetation barriers should help absorb and filter the particulate air pollution.

Table 1. The $\text{PM}_{2.5}$ concentration in the eight districts of Hangzhou by four seasons in 2015, including maximum, minimum, mean and standard deviation value.

		Shangcheng	Xiacheng	Jianggan	Xihu	Gongshu	Binjiang	Yuhang	Xiaoshan
Spring	Max	51.69	58.7	57.11	58.97	59.49	54.13	61.18	68.54
	Min	47.67	49.04	45.38	46.53	48.84	48.26	23.48	41.07
	Mean	50.32	54.1	52.21	51.94	53.87	51.26	47.65	51.8
	Std	0.94	3.06	2.77	2.64	2.54	0.92	10.29	4.61
Summer	Max	28.14	31.95	32.78	34.94	31.76	29.3	33.03	35.95
	Min	24.28	26.79	22.37	23.89	23.4	23.34	10.84	16.69
	Mean	25.87	29.73	27.11	28.43	27.38	25.49	23.31	24.96
	Std	1.02	1.13	2.29	2.27	2.26	1.33	5.36	3.50
Autumn	Max	45.88	46.51	47.77	45.85	45.63	46.06	50.95	59.63
	Min	41.76	43.76	41.9	40.16	42.51	43.41	24.83	40.8
	Mean	44.12	45.27	44.14	43.35	43.96	44.49	39.41	47.33
	Std	1.03	0.67	1.32	1.18	0.68	0.57	6.30	3.40
Winter	Max	57.09	64.74	64.43	65.57	65.42	59.97	66.47	67.97
	Min	53.03	54.21	46.9	48.26	53.83	51.7	44.06	44.06
	Mean	54.67	60.19	54.67	55.14	61.08	54.82	54.63	54.63
	Std	1.06	2.86	4.49	2.61	3.86	1.61	8.56	5.60

Table 2. The area percentage of the different land use type to the total study area percentage (%) by the three class of $\text{PM}_{2.5}$ concentration in the four seasons.

Land use type	Class of $\text{PM}_{2.5}$	Spring (%)	Summer(%)	Autumn(%)	Winter(%)
Grassland	35	0.07	4.59	0.11	0.1
Plowland	35	0.13	11.52	0.25	0.16
Building land	35	0.17	2.51	0.26	0.25
Traffic land	35	0.05	4.92	0.07	0.07
Forest	35	3.49	23.39	3.93	4.35
Water	35	0.03	12.21	0.1	0.05
Orchard	35	0.22	10.87	0.45	0.3

Grassland	35-50	1.84	0.4	3.03	1.57
plowland	35-50	5.27	0.59	6.35	5.23
Building land	35-50	6.74	24.12	14.35	5.73
Road traffic land	35-50	1.41	0.55	3.11	1.38
Forest	35-50	13.76	2.82	15.49	14.81
Water	35-50	6.32	0.6	7.39	3.12
Orchard	35-50	3.89	0.92	4.66	3
Grassland	>50	3.09	0	1.84	3.33
plowland	>50	6.71	0	5.51	6.71
Building land	>50	19.72	0	12.02	20.65
Road traffic land	>50	4.02	0	2.29	4.02
Forest	>50	8.95	0	6.78	7.03
Water	>50	6.46	0	5.32	9.64
Orchard	>50	7.67	0	6.68	8.48

3.4. Population Group Exposure under the Roof of the PM_{2.5}

For the annual mean PM_{2.5} concentration in 2015, the spatial distribution of the population density was 249.18 Pop/km²(±746.53) in PM_{2.5} <35µm/m³. The distributed area was 266.29km²; between 35~50µm/m³, the density was 1,521.60 Pop/km²(±3,584.08), and the area was 1,483.99km². The population density was 1,582.66 Pop/km²(±3,124.79) for > 50µm/m³ and the area was 1,188.18km². The result of these calculations determined the population mainly distributed in the high PM_{2.5} concentration, where land surface also covered high density buildings. On the other hand, gaseous and particulate pollutants were also exposed due to human activity. Pollution from human activities has severely contributed to huge health impacts on mankind over a long period of time [65-67]. Considering the special group of infants and juveniles attending school, the younger individuals are less resistant to disease and daily exposure to the high PM_{2.5} concentration can cause both current and future health problems. It is very important to pay attention to this group of individuals and closely monitor their state of health at all times.

In the study area, in 2015, the number of kindergarten institutions equaled 623 and the respective number of infants equaled 239,459; the number of

primary school institutions equaled 265 while the number of respective students equaled 389,260; and the number of middle school institutions equaled 123 while the number of respective students equaled 217,959. By the different PM_{2.5} concentration class, 294 kindergarten students distributed PM_{2.5}> 50 ug/m³, 325 distributed 35~50 ug/m³, and only four distributed <35 ug/m³. Seven primary schools distributed < 35 ug/m³; 147 distributed between 35~50 ug/m³, and 111 distributed >50 ug/m³. Two middle schools distributed < 35 ug/m³, 123 middle schools distributed between 35~50 ug/m³, and 71 middle schools distributed >50 ug/m³ (Figure. 6, Table 3). These results concluded that at each of the aforementioned educational levels, only 1.66% (14,055) of infants and juveniles involved in the study lived in an environment that met the national air quality standard. This number was even below the national mean level, who living environment reached China's National Air Quality Standard for Grade II [13, 27, 68]. In addition, 41.97% (355,333) of infants and juveniles lived in a heavily polluted environment (PM_{2.5} > 50 ug/m³), and 56.49% (478,257) of infants and juveniles lived in an intermediately polluted environment (PM_{2.5} between 35~ 50 ug/m³), shown in the study area (Table 3). Although we only achieved statistics for the number of infants and juveniles by these three levels of schooling, their families and the schools near their

residential areas experience a similar atmospheric environment. Although children's disease attributed by PM_{2.5} exposure was not separately studied, additional findings showed that China's leading mortality causes (stroke, IHD, LC, and COPD) could be attributed to PM_{2.5} exposure to some extent [36, 69-71]. Considering the lag health effects of long-term PM_{2.5} exposure, it is necessary to track the health status of infants and juveniles from now until they have entered into adulthood. In doing so, we can more effectively eliminate the harm PM_{2.5} poses to our overall health.

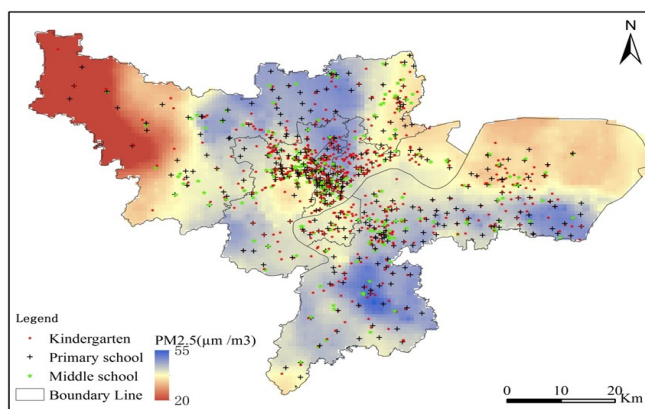


Figure 6. The Kindergarten, Primary and middle school distributed in the annual mean PM_{2.5} concentration.

Table 3 The number of Kindergarten, Primary School and the Middle Schools by the three class of annual PM_{2.5} concentration and the population density.

PM _{2.5} (ug/m ³)	Kindergarten	Primary School	Middle School
35	4	7	2
50	325	147	123
>50	294	111	71
Total School	623	265	195
Total population	239459	389260	217959
Mean (Pop/School)	384	1469	1118

4. CONCLUSION

We used a combination of the dispersed monitoring sites data, land use data, and MODIS remote-sensing AOT to calculate the inversion of PM_{2.5} concentration and its effects on the general population and students in Hangzhou in 2015. From our research, we were able to draw the following conclusions.

First, the seasonal variation characteristics of PM_{2.5} concentration distribution was as follows: winter > spring > autumn > summer. For the eight main urban districts, the highest average value PM_{2.5} concentration in spring, summer, and autumn all showed in the Xiacheng district, and the lowest value showed in the Yuhang district. However, in winter, the highest average value showed in the Gongshu district, and the lowest value also showed in the Yuhang district. In addition, the lowest value in all four seasons appeared in the Yuhang district.

Secondly, for the different land use types, we found that in winter and spring, 59.86% and 56.62% of the land area showed the PM_{2.5} >50µg/m³, respectively. Among the building area, we accounted for 20.65% in winter and 19.72% in spring. In autumn, 54.38% of the land area exposure equaled PM_{2.5} 35~50µg/m³, and the forest type accounted for a large proportion (15.49%). In the summer, the air particulate content was lowest. 70.01% of the land surface area equaled PM_{2.5} <35µg/m³, and the forest type accounted for 23.39%. Increasing the forest landscape performs the function of absorbing and filtering the particulate air pollution with the goal of sending the pollution into remission.

Finally, based on the spatial distribution of different class PM_{2.5} concentration, only 9.06% of the population lived in an environment that met the national air quality standards. For infants and juveniles, only 1.66% (14,055) lived in PM_{2.5} <35µg/m³; 56.49%

(478,257) lived in the intermediate pollution environment ($PM_{2.5}$ 35~ 50 $\mu g/m^3$); and 41.97% (355,333) of infants and juveniles lived in a heavy polluted environment ($PM_{2.5} > 50 \mu g/m^3$) in the study area.

We firmly believe that not only in Hangzhou, but also spanning all of China, a devastating number of infants and juveniles currently live in an atmospheric pollution environment; action must be taken and attention must be paid in order to safeguard the future of the country.

ACKNOWLEDGEMENT

Funding: This research was funded by the National Natural Science Foundation of China (No. 41601100), the Strategic Priority Research Program of the Chinese Academy of Sciences (No. XDA19040305, XDA19050501), and National Key Research and Development Program of China (No. 2017YFB0503005), the International Postdoctoral Exchange Fellowship Program 2015 by the Office of China Postdoctoral Council (the approval document number: No: 38 Document of OCPC, 2015).

REFERENCES

- [1] Xie, S. D.; Yu, T.; Zhang, Y. H.; Zeng, L. M.; Qi, L.; Tang, X. Y., Characteristics of PM_{10} , SO_2 , NO , and O_3 in ambient air during the dust storm period in Beijing. *Sci Total Environ* 2005, 345, (1-3), 153-164. PMID:15919536 [View Article](#) [PubMed/NCBI](#)
- [2] Edwards, R., Smog blights babies in the womb. *New Sci* 1996, 152, (2052), 4-4.
- [3] Dockery, D. W., Epidemiologic-Study Design for Investigating Respiratory Health-Effects of Complex Air-Pollution Mixtures. *Environ Health Persp* 1993, 101, 187-191. PMID:8206028 PMCid:PMC1519696
- [4] Pope, C. A.; Burnett, R. T.; Turner, M. C.; Cohen, A.; Krewski, D.; Jerrett, M.; Gapstur, S. M.; Thun, M. J., Lung Cancer and Cardiovascular Disease Mortality Associated with Ambient Air Pollution and Cigarette Smoke: Shape of the Exposure-Response Relationships. *Environ Health Persp* 2011, 119, (11), 1616-1621. PMID:21768054 PMCid:PMC3226505 [View Article](#) [PubMed/NCBI](#)
- [5] Lim, S. S.; Vos, T.; Flaxman, A. D.; Danaei, G.; Shibuya, K.; Adair-Rohani, H.; Amann, M.; Anderson, H. R.; Andrews, K. G.; Aryee, M.; Atkinson, C.; Bacchus, L. J.; Bahalim, A. N.; Balakrishnan, K.; Balmes, J.; Barker-Collo, S.; Baxter, A.; Bell, M. L.; Blore, J. D.; Blyth, F.; Bonner, C.; Borges, G.; Bourne, R.; Boussinesq, M.; Brauer, M.; Brooks, P.; Bruce, N. G.; Brunekreef, B.; Bryan-Hancock, C.; Bucello, C.; Buchbinder, R.; Bull, F.; Burnett, R. T.; Byers, T. E.; Calabria, B.; Carapetis, J.; Carnahan, E.; Chafe, Z.; Charlson, F.; Chen, H. L.; Chen, J. S.; Cheng, A. T. A.; Child, J. C.; Cohen, A.; Colson, K. E.; Cowie, B. C.; Darby, S.; Darling, S.; Davis, A.; Degenhardt, L.; Dentener, F.; Des Jarlais, D. C.; Devries, K.; Dherani, M.; Ding, E. L.; Dorsey, E. R.; Driscoll, T.; Edmond, K.; Ali, S. E.; Engell, R. E.; Erwin, P. J.; Fahimi, S.; Falder, G.; Farzadfar, F.; Ferrari, A.; Finucane, M. M.; Flaxman, S.; Fowkes, F. G. R.; Freedman, G.; Freeman, M. K.; Gakidou, E.; Ghosh, S.; Giovannucci, E.; Gmel, G.; Graham, K.; Grainger, R.; Grant, B.; Gunnell, D.; Gutierrez, H. R.; Hall, W.; Hoek, H. W.; Hogan, A.; Hosgood, H. D.; Hoy, D.; Hu, H.; Hubbell, B. J.; Hutchings, S. J.; Ibeanusi, S. E.; Jacklyn, G. L.; Jasrasaria, R.; Jonas, J. B.; Kan, H. D.; Kanis, J. A.; Kassebaum, N.; Kawakami, N.; Khang, Y. H.; Khatibzadeh, S.; Khoo, J. P.; Kok, C.; Laden, F.; Lalloo, R.; Lan, Q.; Lathlean, T.; Leasher, J. L.; Leigh, J.; Li, Y.; Lin, J. K.; Lipshultz, S. E.; London, S.; Lozano, R.; Lu, Y.; Mak, J.; Malekzadeh, R.; Mallinger, L.; Marcenes, W.; March, L.; Marks, R.; Martin, R.; McGale, P.; McGrath, J.; Mehta, S.; Mensah, G. A.; Merriam, T. R.; Micha, R.; Michaud, C.; Mishra, V.; Hanafiah, K. M.; Mokdad, A. A.; Morawska, L.; Mozaffarian, D.; Murphy, T.; Naghavi, M.; Neal, B.; Nelson, P. K.; Nolla, J. M.; Norman, R.; Olives, C.; Omer, S. B.; Orchard, J.; Osborne, R.; Ostro, B.; Page, A.; Pandey, K. D.; Parry, C. D. H.; Passmore, E.; Patra, J.; Pearce, N.; Pelizzari, P. M.; Petzold, M.; Phillips, M. R.; Pope, D.; Pope, C. A.; Powles, J.; Rao, M.; Razavi, H.; Rehfuess, E. A.; Rehm, J. T.; Ritz, B.; Rivara, F. P.; Roberts, T.; Robinson, C.; Rodriguez-Portales, J. A.; Romieu, I.; Room, R.; Rosenfeld, L. C.; Roy, A.; Rushton, L.; Salomon, J. A.; Sampson, U.; Sanchez-Riera, L.; Sanman, E.; Sapkota, A.; Seedat, S.; Shi, P. L.; Shield, K.; Shivakoti, R.; Singh, G. M.; Sleet, D. A.; Smith, E.; Smith, K. R.; Stapelberg, N. J. C.; Steenland, K.; Stockl, H.; Stovner, L. J.; Straif, K.; Straney, L.; Thurston, G. D.; Tran, J. H.; Van Dingenen, R.; van Donkelaar, A.; Veerman, J. L.; Vijayakumar, L.; Weintraub, R.; Weissman, M. M.; White, R. A.; Whiteford, H.; Wiersma, S. T.; Wilkinson, J. D.; Williams, H. C.; Williams, W.; Wilson, N.; Woolf, A. D.; Yip, P.; Zielinski, J. M.; Lopez, A. D.; Murray, C. J. L.; Ezzati, M., A comparative risk assessment of burden of disease and injury attributable to 67 risk factors and risk factor clusters in 21 regions, 1990-2010: a systematic analysis for the Global Burden of Disease Study 2010. *Lancet* 2012, 380, (9859), 2224-2260. 61766-8 [View Article](#)
- [6] Arnold, C., Disease Burdens Associated with $PM_{2.5}$ Exposure How a New Model Provided Global Estimates. *Environ Health Persp* 2014, 122, (4), A111-A111. PMID:24691739 PMCid:PMC3983717 [View Article](#) [PubMed/NCBI](#)
- [7] Burnett, R. T.; Pope, C. A.; Ezzati, M.; Olives, C.; Lim, S. S.; Mehta, S.; Shin, H. H.; Singh, G.; Hubbell, B.; Brauer, M.; Anderson, H. R.; Smith, K. R.; Balmes, J. R.; Bruce, N. G.; Kan, H. D.; Laden, F.; Pruss-Ustun, A.; Michelle, C. T.; Gapstur, S. M.; Diver, W. R.; Cohen, A., An Integrated Risk Function for Estimating the Global Burden of Disease Attributable to Ambient Fine Particulate Matter Exposure. *Environ Health Persp* 2014, 122, (4), 397-403. [View Article](#)
- [8] Lelieveld, J.; Evans, J. S.; Fnais, M.; Giannadaki, D.; Pozzer, A., The contribution of outdoor air pollution sources to premature mortality on a global scale. *Nature* 2015, 525, (7569), 367-+. PMID:26381985 [View Article](#)

cle PubMed/NCBI

[9]Li, L.; Yang, J.; Song, Y. F.; Chen, P. Y.; Ou, C. Q., The burden of COPD mortality due to ambient air pollution in Guangzhou, China. *Sci Rep-Uk* 2016, 6.

[10]Lin, H. L.; Liu, T.; Xiao, J. P.; Zeng, W. L.; Li, X.; Guo, L. C.; Xu, Y. J.; Zhang, Y. H.; Vaughn, M. G.; Nelson, E. J.; Qian, Z. M.; Ma, W. J., Quantifying short-term and long-term health benefits of attaining ambient fine particulate pollution standards in Guangzhou, China. *Atmos Environ* 2016, 137, 38-44. [View Article](#)

[11]Vedal, S., Health effects of inhalable particles: Implications for British Columbia: the ministry. 1995.

[12]Derwent, R.G., EPAQS recommendations—can they be implemented. Paper presented at the proceedings of the 63rd national society for clean Air environmental protection conference and exhibition. National Society for Clean Air, Brighton 1996.

[13]Song, C.; He, J.; Wu, L.; Jin, T.; Chen, X.; Li, R.; Ren, P.; Zhang, L.; Mao, H., Health burden attributable to ambient PM_{2.5} in China. *Environ Pollut* 2017, 223, 575-586. PMID:28169071 [View Article](#) PubMed/NCBI

[14]Kan, H. D.; Chen, R. J.; Tong, S. L., Ambient air pollution, climate change, and population health in China. *Environ Int* 2012, 42, 10-19. PMID:21440303 [View Article](#) PubMed/NCBI

[15]Erismann, J. W.; Draaijers, G., Deposition to forests in Europe: most important factors influencing dry deposition and models used for generalisation. *Environ Pollut* 2003, 124, (3), 379-388. 00049-6 [View Article](#)

[16]Sabin, L. D.; Lim, J. H.; Stolzenbach, K. D.; Schiff, K. C., Atmospheric dry deposition of trace metals in the coastal region of Los Angeles, California, USA. *Environ Toxicol Chem* 2006, 25, (9), 2334-2341. PMID:16986787 [View Article](#) PubMed/NCBI

[17]Chen, J. Q.; Zhu, L. Y.; Fan, P.; Tian, L.; Laforteza, R., Do green spaces affect the spatiotemporal changes of PM_{2.5} in Nanjing? *Ecological Processes* 2016, 5, (7), 1-13

[18]Rohde, R. A.; Muller, R. A., Air Pollution in China: Mapping of Concentrations and Sources. *Plos One* 2015, 10, (8). [View Article](#)

[19]Wu, Y.; Zhang, S. J.; Li, M. L.; Ge, Y. S.; Shu, J. W.; Zhou, Y.; Xu, Y. Y.; Hu, J. N.; Liu, H.; Fu, L. X.; He, K. B.; Hao, J. M., The challenge to NO_x emission control for heavy-duty diesel vehicles in China. *Atmos Chem Phys* 2012, 12, (19), 9365-9379. [View Article](#)

[20]Wang, S. X.; Zhao, B.; Cai, S. Y.; Klimont, Z.; Nielsen, C. P.; Morikawa, T.; Woo, J. H.; Kim, Y.; Fu, X.; Xu, J. Y.; Hao, J. M.; He, K. B., Emission trends and mitigation options for air pollutants in East Asia. *Atmos Chem Phys* 2014, 14, (13), 6571-6603. [View Article](#)

[21]Zhao, B.; Wang, S. X.; Liu, H.; Xu, J. Y.; Fu, K.; Klimont, Z.; Hao, J. M.; He, K. B.; Cofala, J.; Amann, M., NO_x emissions in China: historical trends and future perspectives. *Atmos Chem Phys* 2013, 13, (19), 9869-9897. [View Article](#)

[22]van Donkelaar, A.; Martin, R. V.; Brauer, M.; Kahn, R.; Levy, R.; Verduzco, C.; Villeneuve, P. J., Global Estimates of Ambient Fine Particulate Matter Concentrations from Satellite-Based Aerosol Optical Depth: Development and Application. *Environ Health Persp* 2010, 118, (6), 847-855. PMID:20519161 PMCid:PMC2898863 [View Article](#) PubMed/NCBI

[23]Apte, J. S.; Marshall, J. D.; Cohen, A. J.; Brauer, M.,

Addressing Global Mortality from Ambient PM_{2.5}. *Environ Sci Technol* 2015, 49, (13), 8057-8066. PMID:26077815 [View Article](#) PubMed/NCBI

[24]Van Donkelaar, A.; Martin, R. V.; Brauer, M.; Kahn, R.; Levy, R.; Verduzco, C.; Villeneuve, P. J., Global Estimates of Ambient Fine Particulate Matter Concentrations from Satellite-based Aerosol Optical Depth: Development and Application. In University of British Columbia 2015.

[25]Ma, Z. W.; Hu, X. F.; Sayer, A. M.; Levy, R.; Zhang, Q.; Xue, Y. G.; Tong, S. L.; Bi, J.; Huang, L.; Liu, Y., Satellite-Based Spatiotemporal Trends in PM_{2.5} Concentrations: China, 2004-2013. *Environ Health Persp* 2016, 124, (2), 184-192. PMID:26220256 PMCid:PMC4749081 [View Article](#) PubMed/NCBI

[26]West, J. J.; Cohen, A.; Dentener, F.; Brunekreef, B.; Zhu, T.; Armstrong, B.; Bell, M. L.; Brauer, M.; Carmichael, G.; Costa, D. L.; Dockery, D. W.; Kleeman, M.; Krzyzanowski, M.; Kunzli, N.; Liou, S. C.; Lung, S. C. C.; Martin, R. V.; Poschl, U.; Pope, C. A.; Roberts, J. M.; Russell, A. G.; Wiedinmyer, C., "What We Breathe Impacts Our Health: Improving Understanding of the Link between Air Pollution and Health". *Environ Sci Technol* 2016, 50, (10), 4895-4904. PMID:27010639 [View Article](#) PubMed/NCBI

[27]Liu, M. M.; Huang, Y. N.; Ma, Z. W.; Jin, Z.; Liu, X. Y.; Wang, H.; Liu, Y.; Wang, J. N.; Jantunen, M.; Bi, J.; Kinney, P. L., Spatial and temporal trends in the mortality burden of air pollution in China: 2004-2012. *Environ Int* 2017, 98, 75-81. PMID:27745948 PMCid:PMC5479577 [View Article](#) PubMed/NCBI

[28]Janhall, S., Review on urban vegetation and particle air pollution - Deposition and dispersion. *Atmos Environ* 2015, 105, 130-137. [View Article](#)

[29]Li, C. C. M.; J. T.; Lau, A. K.; et al, Application of MODIS aerosol product in the study of air pollution in Beijing. *Science in China: Earth Science* 2005, 35, 177 - 186.

[30]Lee, H. J.; Liu, Y.; Coull, B. A.; Schwartz, J.; Koutrakis, P., A novel calibration approach of MODIS AOD data to predict PM_{2.5} concentrations. *Atmos. Chem. Phys.* 2011, 11, (15), 7991-8002. [View Article](#)

[31]Tao, J.; Zhang, M.; Chen, L.; Wang, Z.; Su, L.; Ge, C.; Han, X.; Zou, M., A method to estimate concentrations of surface-level particulate matter using satellite-based aerosol optical thickness. *Sci. China Earth Sci.* 2013, 56, (8), 1422-1433. [View Article](#)

[32]Strandgren, J., Study of Satellite Retrieved Aerosol Optical Depth Spatial Resolution Effect on Particulate Matter Concentration Prediction. Luleå University of Technology, , 2014. [View Article](#)

[33]Paciorek, C. J.; Liu, Y., Limitations of Remotely Sensed Aerosol as a Spatial Proxy for Fine Particulate Matter. *Environmental Health Perspectives* 2009, 117, (6), 904-909. PMID:19590681 PMCid:PMC2702404 [View Article](#) PubMed/NCBI

[34]Brauer, M.; Amann, M.; Burnett, R. T.; Cohen, A.; Dentener, F.; Ezzati, M.; Henderson, S. B.; Krzyzanowski, M.; Martin, R. V.; Van Dingenen, R.; van Donkelaar, A.; Thurston, G. D., Exposure Assessment for Estimation of the Global Burden of Disease Attributable to Outdoor Air Pollution. *Environ Sci Technol* 2012, 46, (2), 652-660. PMID:22148428 PMCid:PMC4043337 [View Article](#) PubMed/NCBI

- [35]Ma, Z. W.; Hu, X. F.; Huang, L.; Bi, J.; Liu, Y., Estimating Ground-Level PM_{2.5} in China Using Satellite Remote Sensing. *Environ Sci Technol* 2014, 48, (13), 7436-7444. PMID:24901806 [View Article](#) [PubMed/NCBI](#)
- [36]Cao, J. J.; Shen, Z. X.; Chow, J. C.; Qi, G. W.; Watson, J. G., Seasonal variations and sources of mass and chemical composition for PM₁₀ aerosol in Hangzhou, China. *Particuology* 2009, 7, (3), 161-168. [View Article](#)
- [37]Bai, H. Z.; Zhang, H. J., Characteristics, sources, and cytotoxicity of atmospheric polycyclic aromatic hydrocarbons in urban roadside areas of Hangzhou, China. *J Environ Sci Heal A* 2015, 52, (4), 303-312. PMID:27925846 [View Article](#) [PubMed/NCBI](#)
- [38]Fu, Q. L.; Mo, Z.; Lyu, D. N.; Zhang, L. F.; Qin, Z. W.; Tang, Q. M.; Yin, H. F.; Xu, P. W.; Wu, L. Z.; Lou, X. M.; Chen, Z. J.; Yao, K., Air pollution and outpatient visits for conjunctivitis: A case-crossover study in Hangzhou, China. *Environ Pollut* 2017, 231, 1344-1350. PMID:28947318 [View Article](#) [PubMed/NCBI](#)
- [39]Hong, S. M.; Jiao, L.; Ma, W. L., Variation of PM_{2.5} concentration in Hangzhou, China. *Particuology* 2013, 11, (1), 55-62. [View Article](#)
- [40]Jansen, R. C.; Shi, Y.; Chen, J. M.; Hu, Y. J.; Xu, C.; Hong, S. M.; Li, J.; Zhang, M., Using hourly measurements to explore the role of secondary inorganic aerosol in PM_{2.5} during haze and fog in Hangzhou, China. *Adv Atmos Sci* 2014, 31, (6), 1427-1434. [View Article](#)
- [41]Jin, Q.; Gong, L. K.; Liu, S. Y.; Ren, R., Assessment of trace elements characteristics and human health risk of exposure to ambient PM_{2.5} in Hangzhou, China. *Int J Environ Res Public Health* 2017, 14, (10), 983-1002. [View Article](#)
- [42]Liu, G.; Li, J. H.; Wu, D.; Xu, H., Chemical composition and source apportionment of the ambient PM_{2.5} in Hangzhou, China. *Particuology* 2015, 18, 135-143. [View Article](#)
- [43]Liu, H. N.; Ma, W. L.; Qian, J. L.; Cai, J. Z.; Ye, X. M.; Li, J. H.; Wang, X. Y., Effect of Urbanization on the Urban Meteorology and Air Pollution in Hangzhou. *J Meteorol Res-Proc* 2015, 29, (6), 950-965. [View Article](#)
- [44]Lu, H.; Wang, S. S.; Wu, Z. L.; Yao, S. L.; Han, J. Y.; Tang, X. J.; Jiang, B. Q., Variations of polycyclic aromatic hydrocarbons in ambient air during haze and non-haze episodes in warm seasons in Hangzhou, China. *Environ Sci Pollut Res* 2017, 24, (1), 135-145. PMID:27475434 [View Article](#) [PubMed/NCBI](#)
- [45]Lu, H.; Zhu, L. Z.; Chen, S. G., Pollution level, phase distribution and health risk of polycyclic aromatic hydrocarbons in indoor air at public places of Hangzhou, China. *Environ Pollut* 2008, 152, (3), 569-575. PMID:17698267 [View Article](#) [PubMed/NCBI](#)
- [46]Wu, J.; Xu, C.; Wang, Q. Z.; Cheng, W., Potential Sources and Formations of the PM_{2.5} Pollution in Urban Hangzhou. *Atmosphere-Basel* 2016, 7, (8). [View Article](#)
- [47]Xiao, Z. M.; Zhang, Y. F.; Hong, S. M.; Bi, X. H.; Jiao, L.; Feng, Y. C.; Wang, Y. Q., Estimation of the Main Factors Influencing Haze, Based on a Long-term Monitoring Campaign in Hangzhou, China. *Aerosol Air Qual Res* 2011, 11, (7), 873-882. [View Article](#)
- [48]Yu, S. C.; Zhang, Q. Y.; Yan, R. C.; Wang, S.; Li, P. F.; Chen, B. X.; Liu, W. P.; Zhang, X. Y., Origin of air pollution during a weekly heavy haze episode in Hangzhou, China. *Environ Chem Lett* 2014, 12, (4), 543-550. [View Article](#)
- [49]Zhang, G.; Xu, H. H.; Qi, B.; Du, R. G.; Gui, K.; Wang, H. L.; Jiang, W. T.; Liang, L. L.; Xu, W. Y., Characterization of atmospheric trace gases and particulate matter in Hangzhou, China. *Atmos Chem Phys* 2018, 18, (3), 1705-1728. [View Article](#)
- [50]Zheng, S.; Zhou, X. Y.; Singh, R. P.; Wu, Y. Z.; Ye, Y. M.; Wu, C. F., The Spatiotemporal Distribution of Air Pollutants and Their Relationship with Land-Use Patterns in Hangzhou City, China. *Atmosphere-Basel* 2017, 8, (6). [View Article](#)
- [51]Kaufman, Y. J.; Sendra, C., Algorithm for automatic atmospheric corrections to visible and near-IR satellite imagery. *Int J Remote Sens* 1988, 9, (8), 1357-1381. [View Article](#)
- [52]Kaufman, Y. J.; Tanre, D.; Remer, L. A.; Vermote, E. F.; Chu, A.; Holben, B. N., Operational remote sensing of tropospheric aerosol over land from EOS moderate resolution imaging spectroradiometer. *J Geophys Res-Atmos* 1997, 102, (D14), 17051-17067. [View Article](#)
- [53]Hsu, N. C.; Tsay, S. C.; King, M. D.; Herman, J. R., Aerosol properties over bright-reflecting source regions. *Ieee T Geosci Remote* 2004, 42, (3), 557-569. [View Article](#)
- [54]Hsu, N. C.; Tsay, S. C.; King, M. D.; Herman, J. R., Deep blue retrievals of Asian aerosol properties during ACE-Asia. *Ieee T Geosci Remote* 2006, 44, (11), 3180-3195. [View Article](#)
- [55]Levy, R. C.; Remer, L. A.; Kleidman, R. G.; Mattoo, S.; Ichoku, C.; Kahn, R.; Eck, T. F., Global evaluation of the Collection 5 MODIS dark-target aerosol products over land. *Atmos Chem Phys* 2010, 10, (21), 10399-10420. [View Article](#)
- [56]Levy, R. C.; Remer, L. A.; Mattoo, S.; Vermote, E. F.; Kaufman, Y. J., Second-generation operational algorithm: Retrieval of aerosol properties over land from inversion of Moderate Resolution Imaging Spectroradiometer spectral reflectance. *J Geophys Res-Atmos* 2007, 112, (D13). [View Article](#)
- [57]Liu, M. M.; Huang, Y. N.; Jin, Z.; Ma, Z. W.; Liu, X. Y.; Zhang, B.; Liu, Y.; Yu, Y.; Wang, J. N.; Bi, J.; Kinney, P. L., The nexus between urbanization and PM_{2.5} related mortality in China. *Environ Pollut* 2017, 227, 15-23. PMID:28454017 [View Article](#) [PubMed/NCBI](#)
- [58]Gao, L. N.; Zhang, R. J.; Han, Z. W.; Fu, C. B.; Yan, P.; Wang, T. J.; Hong, S. M.; Jiao, L., A Modeling Study of a Typical Winter PM_{2.5} Pollution Episode in a City in Eastern China. *Aerosol Air Qual Res* 2014, 14, (1), 311-322. [View Article](#)
- [59]Ming, L. L.; Jin, L.; Li, J.; Fu, P. Q.; Yang, W. Y.; Liu, D.; Zhang, G.; Wang, Z. F.; Li, X. D., PM_{2.5} in the Yangtze River Delta, China: Chemical compositions, seasonal variations, and regional pollution events. *Environ Pollut* 2017, 223, 200-212. PMID:28131471 [View Article](#) [PubMed/NCBI](#)
- [60]Mehmood, K.; Chang, S. C.; Yu, S. C.; Wang, L. Q.; Li, P. F.; Li, Z.; Liu, W. P.; Rosenfeld, D.; Seinfeld, J. H., Spatial and temporal distributions of air pollutant emissions from open crop straw and biomass burnings in China from 2002 to 2016. *Environ Chem Lett* 2018, 16, (1), 301-309. [View Article](#)
- [61]Ni, Z. Z.; Luo, K.; Zhang, J. X.; Feng, R.; Zheng, H. X.; Zhu, H. R.; Wang, J. F.; Fan, J. R.; Gao, X.; Cen, K. F.,

Assessment of winter air pollution episodes using long-range transport modeling in Hangzhou, China, during World Internet Conference, 2015. *Environ Pollut* 2018, 236, 550-561. PMID:29428709 [View Article](#) [PubMed/NCBI](#)

[62]Zhang, X. M.; Xue, Z. G.; Li, H.; Yan, L.; Yang, Y.; Wang, Y.; Duan, J. C.; Li, L.; Chai, F. H.; Cheng, M. M.; Zhang, W. Q., Ambient volatile organic compounds pollution in China. *Journal of Environmental Sciences* 2017, 55, 69-75. PMID:28477835 [View Article](#) [PubMed/NCBI](#)

[63]Xu, H. D., B.; Zhou, X.; Wang, Q., Effect of fog on urban boundary layer and environment. *J Appl Meteorol Sci* 2002, 13, 170-176.

[64]Wu, Z. P. W., C.; Hou, X.J.; Yang, W.W., Variation of air PM_{2.5} concentration in six urban greenlands. *J Anhui Agri Univ* 2008, 35, 494-498.

[65]Chang, C. J.; Yang, H. H.; Chang, C. A.; Tsai, H. Y., Relationship between Air Pollution and Outpatient Visits for Nonspecific Conjunctivitis. *Invest Ophth Vis Sci* 2012, 53, (1), 429-433. PMID:22205603 [View Article](#) [PubMed/NCBI](#)

[66]Shen, Y.; Wu, Y. Y.; Chen, G. D.; Van Grinsven, H. J. M.; Wang, X. F.; Gu, B. J.; Lou, X. M., Non-linear increase of respiratory diseases and their costs under severe air pollution. *Environ Pollut* 2017, 224, 631-637. PMID:28258857 [View Article](#) [PubMed/NCBI](#)

[67]Mimura, T.; Ichinose, T.; Yamagami, S.; Fujishima, H.; Kamei, Y.; Goto, M.; Takada, S.; Matsubara, M., Air-

borne particulate matter (PM_{2.5}) and the prevalence of allergic conjunctivitis in Japan. *Sci Total Environ* 2014, 487, 493-499. PMID:24802272 [View Article](#) [PubMed/NCBI](#)

[68]Liu, J. K.; Mo, L. C.; Zhu, L. J.; Yang, Y. L.; Liu, J. T.; Qiu, D. D.; Zhang, Z. M.; Liu, J. L., Removal efficiency of particulate matters at different underlying surfaces in Beijing. *Environ Sci Pollut R* 2016, 23, (1), 408-417. PMID:26308922 [View Article](#) [PubMed/NCBI](#)

[69]Yang, G. H.; Wang, Y.; Zeng, Y. X.; Gao, G. F.; Liang, X. F.; Zhou, M. G.; Wan, X.; Yu, S. C.; Jiang, Y. H.; Naghavi, M.; Vos, T.; Wang, H. D.; Lopez, A. D.; Murray, C. J. L., Rapid health transition in China, 1990-2010: findings from the Global Burden of Disease Study 2010. *Lancet* 2013, 381, (9882), 1987-2015. 61097-1 [View Article](#)

[70]Yin, P.; Brauer, M.; Cohen, A.; Burnett, R. T.; Liu, J. M.; Liu, Y. N.; Zhou, M. G., Ambient fine particulate matter exposure and cardiovascular mortality in China: a prospective cohort study. *Lancet* 2015, 386, 6-6. 00584-X [View Article](#)

[71]Guan, W. J.; Zheng, X. Y.; Chung, K. F.; Zhong, N. S., Impact of air pollution on the burden of chronic respiratory diseases in China: time for urgent action. *Lancet* 2016, 388, (10054), 1939-1951. 31597-5 [View Article](#)